Radial void fraction measurement of a random multisized pebble stacking

J. P. Groen

August 28, 2009

Preface

This thesis represents my graduation work for the Bachelor in Applied Physics at Delft University of Technology (DUT). The thesis work was performed in the section Physics of Nuclear Reactors (PNR) of the faculty of Applied Sciences. The research has been supervised by dr. ir. J.L. Kloosterman.
I would like to thank everybody at PNR for their support and suggestions.

Abstract

This report describes the research regarding the radial void fraction of a pebble-bed reactor. The experimental model is a scaled version (1:10) of the active HTR-10 reactor in China. In a pebble-bed reactor the void fraction distribution is important in calculating the correct criticality. In the near wall region the radial void fraction shows an oscillatory behavior named flow channeling. This effect has consequences on the mechanics of heat transfer and on the flow and pressure drop of the coolant through the reactor.Earlier studies have been performed on this topic since their are various ways to determine the porosity profile. In this report the void fraction is acquired using a gamma-transmission technique. With this method the packing fraction can be obtained while keeping the pebble stacking intact.

In the experiments the gamma radiation from the 60 [keV] peak of an Am-241 source is used to determine the decay of the beam through a pebble-bed. Two collimators with a width of 1.0 and 2.0 [mm] are used to create the correct resolution. The measurement time varies from a day to a week, depending on various experimental parameters like the amount of counts and the pebble stacking. Compensating for build up effect was not necessary according to calibration measurements.

The radial void fraction is obtained for different pebble stackings. The profile for an unisized pebble-bed comply with other research. The void fraction distribution of the shaken bed, measured to determine the influence of an earthquake, showed a oscillatory behavior not seen before. The multisized pebble-bed with spheres of two sizes were difficult to produce. Three experiments with a different pebble multisized distribution showed a average void fraction significantly lower than the unisized packed bed. Mixing the smaller spheres in the bed slightly decreased the amplitude of the oscillations. Flow channeling will probably still be observed in a multisized bed. In the experiments uncertainties range from 1% to 10%, dependent on the used collimator and the void fraction. The average void fraction was lower than expected in the multisized experiments. This could be improved by measuring the background during the measurements of by improving the calibration method. Furthermore a method is developed to determine the walls boundary. It is defined as the point with an distance of 1 [mm] from the point of highest void fraction in the profile. This definition was proven useful according to the experiments.

Contents

Chapter 1

Introduction

The changing climate is a hot topic nowadays. Nations, who signed and ratified the Kyoto Protocol, limit their collective emissions by 5,6%. The European Union is still on target to comply to the protocol. But even with the international will, the amount of fossil fuels is decreasing. Nuclear energy is one of the solutions to replace fossil fuel in the future. In the mean time a few problems like the safety aspect need to be solved. The fear of an accident happening either because of human error or due to a terrorist attack is large. Conventional nuclear power plants need complex defense systems to improve their defense-in-depth. This brings along quite some problems besides increasing the cost of the plant. This complexity makes it difficult to evaluate the safety of a reactor. Also the chance for human error could be larger with these complex systems. Modern plants, the so called Generation IV reactors [1], are designed to decrease these problems.

1.1 Pebble-bed reactors

One of the six main Generation IV reactors types is the Very High Temperature Reactor (VHTR) which uses graphite moderation and operates at temperatures around 950 °C. The core can be build of prismatic blocks like the HTTR (High Temperature Engineering Test Reactor) in Japan [2] and the Gas Turbine-Modular Helium Reactor (GT-MHR) of GA (General Atomics) [3]. The core can also consists of a pebble-bed like the HTR-10 (High Temperature Reactor (10MWt)) in China [4] or the PBMR in South Africa [5]. In pebble-bed reactors the nuclear fuel is contained in pebbles of graphite. The graphite pebbles with a diameter of typically 60 mm contain about 5000 to 20.000 coated TRISO particles [6]. These TRISO particles contain a fuel kernel of UO2.
The pebble-bed reactor has two major advantages. The first one is because the reactor can be cooled with an inert gas like helium. An inert gas is not reactive under normal circumstances and the gas does not get radioactive like water, which is used in conventional PWR. Secondly, because of the higher operating temperature of the reactor the energy conversion efficiency improves. The low power density and

high temperature resistance of the core materials ensure that any decay heat will be dissipated and transported to the environment without causing a meltdown.
In Germany a pebble-bed reactor, the AVR (working group test reactor) was built in the sixties to serve as a showcase experimental reactor and as a showcase to how safe this new form of technology was. However in the year 1988, after 21 years of service, the reactor was shutdown in the aftermath of the Chernobyl disaster and operating problems at the reactor. Currently there is one working prototype of the pebble-bed reactor in China, the so called HTR-10. Multiple pebble-bed reactors are being designed for construction in South Africa to supply a large part of their energy needs and accepting pebble-bed reactors as a solution to their growing energy consumption.

1.2 Previous work

Global research of porosity profile An overview of previous work, in compliance with the research of this topic will be found in Chapter 2.

Research at Delft University of Technology This thesis is the fourth on the topic of pebble-beds, being researched at PNR at the Delft University of Technology. Previous work has been done by A. Ooms [7], E. Webbe [8] and V. van Dijk [9].
The work of Ooms was focused at simulating the packing and movement of pebbles in a bed. She compared different simulation techniques and has performed simulations based on static packing. Her conclusions contain a void fraction of 0.45 which is considered a bit high. She recommended to perform a similar research using a Discrete Element Method (DEM).
E. Webbe continued the computational research of Ooms and used a discrete element method to simulate the radial porosity of unisized and multi-sized spheres. The model of unisized spheres is proven to be accurate compared to experimental research with a standard deviation of 0,7%. The simulation of multi-sized pebbles did not finish as expected but it seems like multisized pebbles will flatten the radial porosity profile.
The work of Van Dijk was pure experimental, using a setup called the PEbble Bed EXperiment (PebBEx). The goal was to make a scaled version of the HTR-10 reactor in China [4]. A setup has been developed to measure void fractions using gamma-ray tomography, a non invasive method. After this development was completed, he measured the void fraction for unisized spheres as a function of the radius of the cylinder. His results are in agreement with the model of Webbe and other experimental results. He recommended to further develop the experimental setup. Further research could be done on the porosity profile of pebbles with different size or form of the pebbles.
This thesis will continue the research, using the conclusions and recommendations of Van Dijk. All of the research has been, and is being, supervised by dr.ir. J.L.

Kloosterman. The PebBEx facility has been realized with the assistance of drs. ing. A. Winkelman.

1.3 Research aim

The focus of this thesis is the measurement of the radial void fraction of a pebble-bed. In experiments done by Van Dijk with roughly the same setup, is found that the void fraction is changing near the wall. In nuclear reactors it is desirable to limit these fluctuations. To decrease the radial dependency of the void fraction some changes at the experimental setup will be done and experiments will be performed of measuring the void fraction when shaking the bed. Another solution of smoothening the void fraction is a pebble-bed with multisized pebbles. Experiments based on this multisized pebble-bed are included in this thesis. Secondary objectives are to measure the influence of a smaller collimator and to develop a way to define the wall of the pebble-bed. This is difficult to determine because a part of the wall is taken into the measurements at the wall due to the collimator thickness.

1.4 Outline of the thesis

An outline of this work is as follows. Chapter 2 will consist of the relevant theoretical theory regarding pebble-bed reactor technology and regarding the gamma transmission tomography, the technique used in the measurements. In chapter 3 the experimental facility used for the measurement will be explained. The possibilities of the facility and the used hardware will be discussed. Chapter 4 will explain the approach to get accurate results from the experiments. Chapter 5 shows the results of the experiments. In this chapter there is room to discuss the way data is interpreted and handled. Finally, the conclusions and recommendations of this work are given in chapter 6.

Chapter 2

Theoretical background

2.1 Pebble-bed reactors

In a packed bed the porosity varies sharply near the wall, since the geometry of packing is interrupted there. Near the wall of the vessel the porosity increases since the spheres must conform the wall's curvature. This variation in porosity distribution has consequences for the gas flow through the bed. As a result, the flow profile inside a packed bed is distorted near the wall, reaching a maximum in the near-wall region [10]. This phenomenon is known as flow channeling [11]. Flow channeling has a significant impact on heat and mass transfer in packed beds used at thermal systems and reactors. For this reason the porosity distribution is studied in a variety of experiments during years.

Benenati et al. [12] measured radial void fraction by pouring uniformly sized spherical lead shot into a container. Then all the interstices were filled wit a liquid epoxy resin. Upon curing of the resin the solid cylinder was machined in stages to successively smaller diameters. The weight and diameter were measured for each cut resulting in a radial variation of the void fraction. Bedenig [13] designed his experiments by filling the pebble-bed slowly with water. The relation between the water input and the water level in the bed resulted in a porosity profile from the bottom of the pebble-bed. Pillai [14] made an perspex bed with an measuring grid on the outside of the bed. The number of particles having their centers between the grid lines were counted, this data determined the void fraction distribution at the surface. Goodling et al. [15] made for their research a pebble-bed by pouring polystyrene spheres into a pipe and then filling it up with an epoxy mixed with iron. By weighting the amount of epoxy of each annular ring the void fraction of each radius could be determined. Mueller [16]in contrast used specially fabricated spheres with a metal core. By using X-ray radiography the centers of the spheres in the bed were determined, describing the radial void fraction of the bed. His results were compared with earlier experiments seen in figure 2.1. Van Dijk [9] used a gamma ray tomography technique (roughly the same setup as in this report) to

establish the radial void fraction of a pebble-bed.

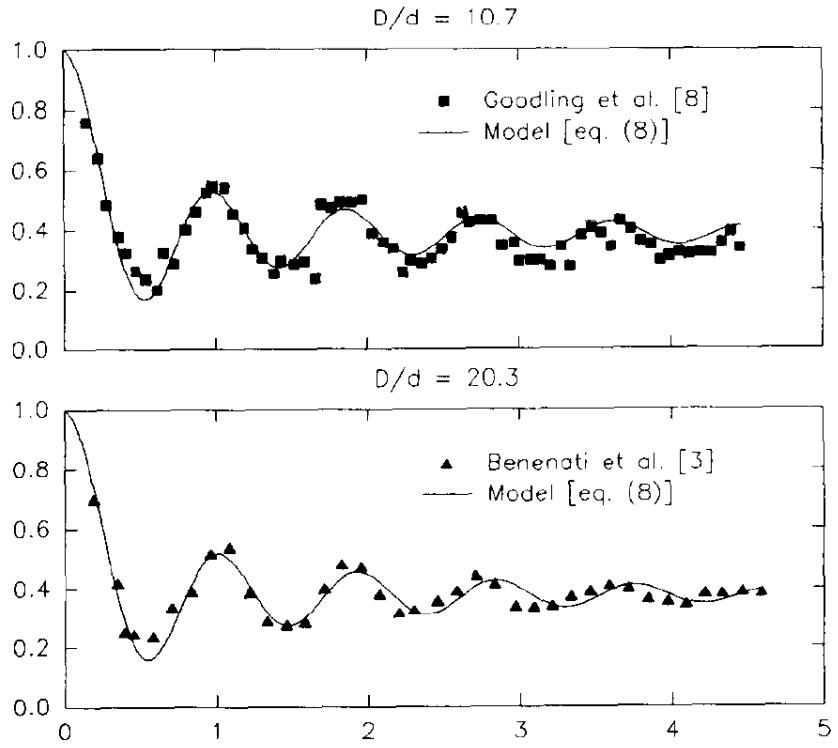

Figure 2.1: Porosity profile of the numerical analysis of Mueller compared to the measurements of Goodling (above) and Benenati (below)

As can be seen in the figures and conclusions of former experiments, the oscillations of the radial void fraction usually damp out at about four to five sphere diameters from the wall.

2.2 Gamma-transmission technique

A gamma ray transmission measurement is a accurate method for measuring void-fractions. In a basic assembly of this technique a gamma emitting source is placed on top of the sample. Between the detector and the sample is a collimator to narrow the gamma ray beam to increase the resolution. On the other side of the sample is a mounting device for a detector. If the sample contains a material with linear attenuation coefficient μ the intensity of the gamma ray beam is given by

$$I = I_0 e^{-\mu d} \tag{2.1}$$

where I_0 is the measured intensity in vacuum and d the thickness of the material in the bed. In a pebble-bed, which contains acrylic spheres and air, equation 2.1 expands to

$$I = I_0 e^{-\mu_m d_m} e^{-(\mu_{air} d_{air} + \mu_{acry} d_{acry})} \tag{2.2}$$

where μ_m,μ_{air} and μ_{acry} are respectively the linear attenuation coefficient of the pebble-bed environment,air and acrylic. To determine the packing fraction, two calibration measurements will suffice. One measurement of a completely filled acrylic bed and one of a empty bed. The intensity of these measurements are given by

$$I_{acry} = I_0 e^{-\mu_m d_m} e^{-\mu_{acry} d_{bed}} \tag{2.3}$$

$$I_{air} = I_0 e^{-\mu_m d_m} e^{-\mu_{air} d_{bed}} \tag{2.4}$$

with d_{bed} the height of the pebble-bed. Combining equations (2.2, 2.3, 2.4) gives the relation:

$$\frac{ln(I) - ln(I_{air})}{ln(I_{acry}) - ln(I_{air})} = \frac{d_{acry}}{d} = \alpha \tag{2.5}$$

where α is the packing fraction of the bed. According to equation 2.5 the packing fraction is independent of the intensity of the source,I_0, and of the decrease in intensity due to the environment, $e^{-\mu_m d_m}$. This means that a calibration of two measurements (air and acrylic) will suffice to measure the porosity profile of a pebble-bed. The choice of radioactive source is based on a few aspects. The intensity of the source must be as high as possible to decrease measurement time. There is a limit to the activity of the used source, if the activity is to high extra precautions are needed. Secondly, the intensity of the gamma beam must greatly decrease when measuring through a full pebble-bed to increase the resolution of the measurement. The attenuation coefficient of a material is dependent on the energy of the used gamma beam as can be seen in the figure A.1. This fact makes it important to know the exact energy of the gamma beam.

Chapter 3

Pebble-bed experiment

The PebBEx is built as a scale model of the HTR-10, a nuclear reactor in China. It is build in Q4 of 2007 and Q1 of 2008 at the section Physics of Nuclear Reactors at the Delft University of Technology by Van Dijk [9]. The objective of the facility is to research the stacking of packed beds. It is built in such way to accurately measure the radial void fraction by using gamma tomography. In this section the composition of the setup will be explained.

3.1 Source

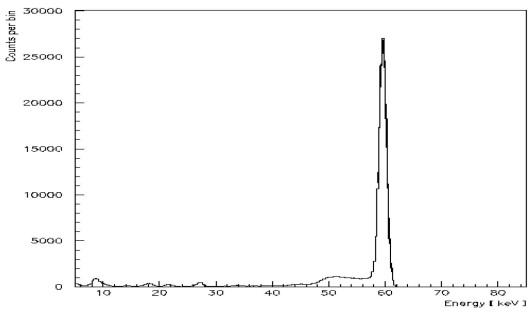

Figure 3.1: Energy spectrum of Am-241

An Am-241 source with an activity of 11.1 [GBq] on 01-01-1968 is used for this experiment. This choice is based on the fact that the Am-241 source emits gamma rays with an energy of 59.5 [keV] [17]. The linear attenuation coefficient of acrylic (PMMA) is 0.2285 [cm^{-1}] [18] at this energy level. This means an decrease of 99% in intensity when measuring through the wall of the vessel. Another reason to use a Am-241 source is that the intensity of the source is higher than other radioactive sources while extra precautions are not necessary [19]. Am-241 emits mostly alpha radiation with an energy of 5.5 [MeV]. To change from an excited state to the ground state gamma radiation with an energy of 59.5 [keV] is produced as can be seen in

the decay scheme of Am-241 (see appendix B). The half life time of 432.2 years guarantees a steady signal during an experiment.

3.2 Collimators

During the experiments two collimators are used. One collimator is made of an circle with an diameter of 1.0 [mm]. This collimator is used for measuring the porosity profile in detail at the wall. The other collimator consists of two half circles with an 2.0 [mm] diameter, connected by a square of 2 by 2 [mm]. Due to the size of the second collimator at the wall of the vessel, a greater segment of the beam will go through the wall. An advantage of the second collimator is that the intensity of the beam is bigger, reducing the uncertainty and time of an experiment. Two holes were made in one ring as can be seen in figure 3.2. The beam will only go through one hole because the detector is not placed in the middle of the setup. The experimental was at first designed for using two detectors [9].

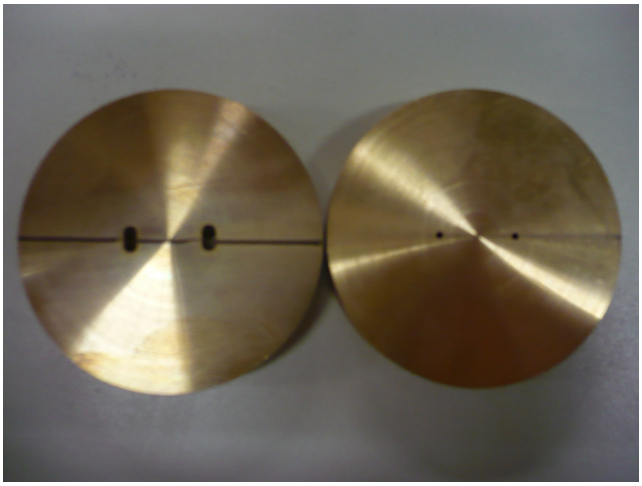

Figure 3.2: The two collimators used in the experiments with. Left the 2 [mm] collimator and right the 1 [mm] collimator.

3.3 Vessel

Because the facility is build as a scaled replica of the HTR-10 there were restrictions to the dimensions of the vessel containing the pebbles. The height/diameter ratio should be 3:2. The used vessel is made of acrylic with a height of 235 [mm], an outer diameter of 240 [mm] and an inner diameter of 228 [mm].The difference in proportions between the HTR-10 and the vessel will not effect the outcomes because the most important factor is the diameter ratio between the vessel and the pebbles. The pebbles used in the experiments are also made of acrylic. This choice is based

on the attenuation coefficient of acrylic. This coefficient leads to an attenuation of the intensity of the gamma beam from 100% to 1% in a completely filled pebble-bed. The pebbles for the first measurements have a diameter of half an inch, 12.7 [mm], leading to a D/d ratio of 18.0. This choice is based on former experiments and on the D/d ratio of the HTR-10. The HTR-10 uses pebbles with a diameter of 6 [cm] in a pebble-bed of 180 [cm] resulting in a D/d ratio of 30.0. This difference in ratio will not affect the wall channeling at the border because in both cases the influence of the other side is negligible [16]. In the multisized packing, 30.000 pebbles with a diameter a quarter of the former one are used i.e. 3.18 [mm]. If the vessel is only filled with these small pebbles, 5% of the bed will be filled.

3.4 Motors

For the measurements two step motors are used. One of the motors rotates the vessel while the other motor translates the setup. The pebble-bed must be rotated to make sure that the radial void fraction can be determined. Due to local variation of the void fraction in the vessel, the setup must be rotated during the whole experiment to average over the radial circumference. This will be carried out by the motor connected to an o-ring belt, surrounding the vessel (figure 3.3) The translating motor moves the setup to measure the next radius of the vessel in steps of 0.5 [mm]

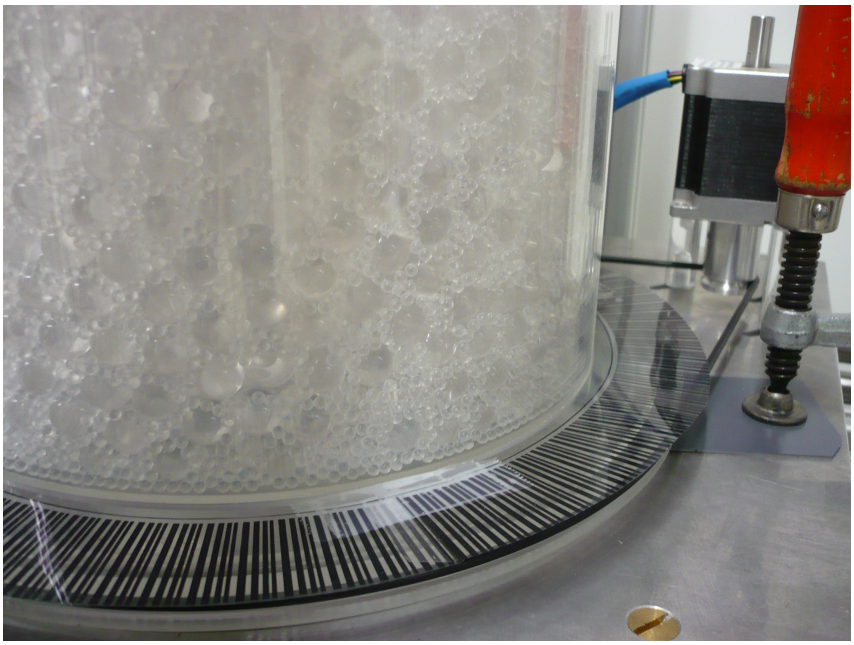

Figure 3.3: The method of rotating the vessel

3.5 Detector

The detector used to measure the gamma rays is a scintillation detector. The crystal in the detector is made of NaI(TI), sodium iodide doped with thallium. With this crystal gamma radiation can easily be detected. A second reason to use an scintillation detector is the possibility to measure the energy of the gamma rays. Without this opportunity the specific peak of Am-241 could not be selected.

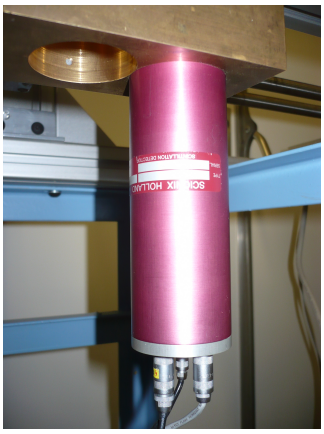

Figure 3.4: The scintillation detector used in the experiments

3.6 Amplifier and windows

Before the pulses of the detector can be analyzed they must first be amplified and filtered to select the 60 [keV] peak of Am-241. The pulses are amplified with a factor 100 by the *Ortec 570* amplifier. After the amplification the pulse voltage range from 0-10 [V]. The peak of Am-241 is selected using a single channel analyzer, *Canberra Model 2030*. In the outcome of the measurements (see section 5.1) an energy window of 1.7-3.7 [V] is selected and an amplification of 100.

Figure 3.5: A picture of the amplifier (second slot) and the SCA (third slot)

3.7 Labview program

Only one Labview program is necessary to make a measurement. The program is developed by Van Dijk and Winkelman. The program consists of different sections (see figure 3.6), the two motors two are controlled in the upper part, while the data after the amplification and filter is gathered and interpreted in the lower part.

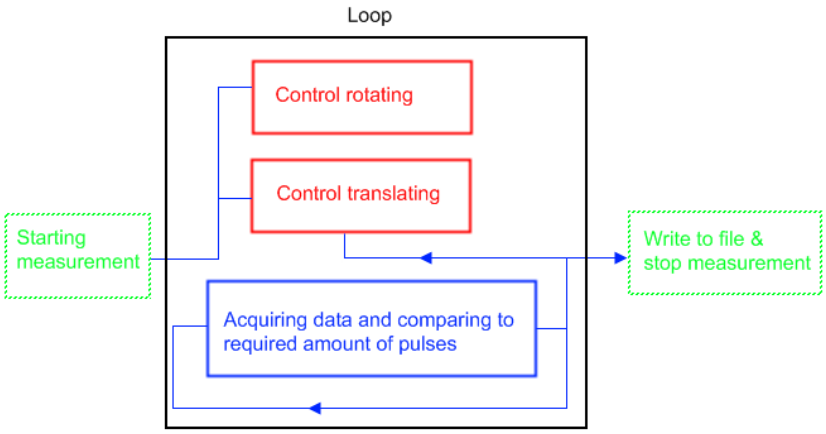

Figure 3.6: Schematic overview of the used Labview program

Chapter 4

Experimental procedure

4.1 Goal

The goal of the experiments is to gain information about the radial void fraction of different pebble stackings. Before the interesting measurements can be performed, information is needed about the different factors influencing the measurements and if the results of the measurements are in agreement with the theory.

4.2 Strategy

To gain information about the porosity profile of a pebble-bed a gamma-ray transmission technique will be used. For this technique two calibration measurements of both mediums in the vessel are required. This will be done for each measurements by starting on the outside of the vessel (calibration of full air). Next, the wall of the vessel is brought between source and detector for the calibration of a packing fraction of 100%. After these calibrations the intensity at the different radii can be measured. The spheres in the pebble-bed can not exceed the height of the vessel.

4.3 Theory

To validate the theory the same strategy is used as done by Van Dijk. The intensity is measured of different acrylic heights by using 20 acrylic discs of 10 [mm]. The radioactive source is placed precisely the same in every measurement. This is necessary due to the variation of beam intensity when rotating the source [9]. Because there were some changes to the setup and the Labview program since the measurements of Van Dijk, new checks have to be performed. The results of this measurement can be seen in section 5.4. If the results are in agreement with theory the measurements of interest can be started.

4.4 Pebble stacking management

Point of interest is the realization of a pebble-bed structure. This is an significant part of the experimental procedure which should be handled with care. The chosen methods directly influence the results of the measurements so it is important to make sure the pebble-bed which is created is in agreement with a pebble-bed reactor like the HTR-10. As stated before, the top surface of the pebble stacking should be uniform at the same height as the height of the vessel.

4.4.1 Filling the vessel

In contrast with Van Dijk the vessel is filled until the top of the vessel is reached. This choice is made to use the calibration method described before (section 4.2). The vessel is filled in different ways in the experiments. It is difficult to achieve an ideally filled multi-sized pebble-stacking. In this section the methods used in the 5 experiments are explained. The obtained multisized pebble-bed stackings are presented in section 5.7.1.

Experiment 1: Unisized pebble-bed In the first experiment the spheres were placed in the vessel rather quickly. The last ones were put in the bed with care.

Experiment 2: Shaken pebble-bed For the shaking experiment, each time a tenth of the total spheres were put in the bed followed by shaking the vessel. From observations, shaking the vessel after completely filling the vessel is not successful due to the mass of all the spheres on top. This will result in only reconfiguration of the top rows of the pebble-bed.

Experiment 3: Multisized pebble-bed 1 The first multisized method consist of randomly put the two types of spheres in the vessel. There were two reasons to try this method. The first reason is to create knowledge about the random distribution of the balls. Secondly, the influence of the other methods with respect to a random bed could be investigated.

Experiment 4: Multisized pebble-bed 2 Secondly the vessel was made by sequentially filling it with the different type of spheres. The gross of the smaller spheres were put within 5 ball diameters of the wall The smaller ones will try to make it to the bottom and fill up the space between the spheres.

Experiment 5: Multisized pebble-bed 3 In the third multisized experiment the vessel was also filled by the method of experiment 4. To create a better distribution of the smaller spheres the vessel had shaken, letting only the small spheres reposition themselves. Although this method is not practical in a pebble-bed reactor it is used because only the influence of the smaller pebbles on the flow channeling is of interest.

4.4.2 Uniform surface

To make sure the pebble-bed height is as uniform as possible a plate will slowly be pushed over the top of the pebble-bed. The surplus of spheres which cannot find a place will be removed from the pebble-bed. It is important to keep the pressure at a minimum to maintain an unpressurized pebble-bed stacking.

4.5 Background influences

The background radiation may greatly influence the measurements. Although the relative radial void fraction will still be recognizable, the background changes the total void fraction of a measurement. That's why it is important to obtain information about the background. During the project the background is measured several times. The first time was during the energy spectrum measurements to see if the energy spectrum of the background had peaks due to hardware. Also during calibration of the experimental setup the background is measured to investigate the influence of perspex on the background. Day-long measurements will be made to check the background over time. Because the void fraction measurements will last several days it is important to check if the background is steady over time. In the facility it is not possible to measure the background during a measurement. The background will be simulated as a constant factor. This background simulation is based on the described background measurements . The results can be found in section 5.3

4.6 Rotating the vessel

During a measurement rotation of the vessel is important. Without rotation the local void fraction will be measured. This void fraction can significantly differ from the radial void fraction according to measurements of Van Dijk [9] and numerical analysis of du Toit [20]. During the measurements of Van Dijk the vessel was rotated on led bullets. This bullets were replaced by three teflon sliding-contact bearings. In the experiments different O-rings will be used because after a few measurements an O-ring is stretched out and will eventually slip if in contact with the motor. The rotation speed is monitored in the experiments by a photodetector. A bar code surrounds the vessel. Every line of the bar code through the detector will cause a pulse. The total count of pulses is an indicator for the rotation speed.

4.7 Defining the wall

The wall will be defined by performing long time measurements for different setups. This measurements will be used to determine the center of the pebble-bed. A MATLAB code is developed to see if the profile is repeating itself. The position of the

wall will be varied to obtain the biggest overlap. This position will be defined as the edge of the pebble-bed. The results of this method can be found in section 5.2.

Chapter 5

Results

5.1 Energy spectrum after amplification

Measurements of the energy spectrum of the source, Am-241, were made. This spectrum is obtained by using a multi-channel analyzer (MCA) provided by F. Geurink of the section Radiation and Isotopes for Health (RIH). Two different spectrum measurements of the source are made, one with an amplification of 100 and an other with an amplification of 300.

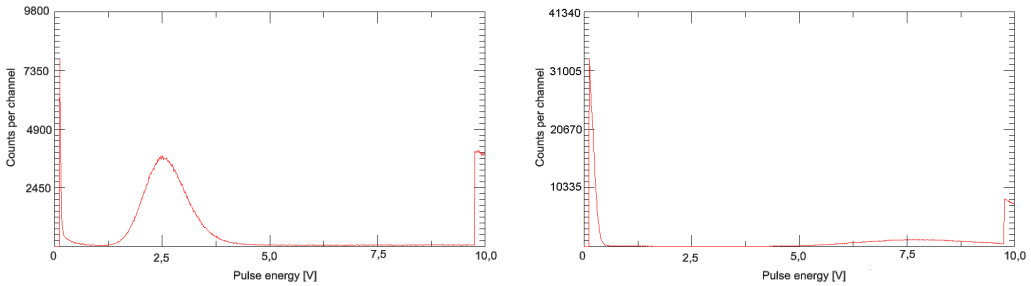

(a) Amplification of 100x

(b) Amplification of 300x

Figure 5.1: Energy spectrum measurements of the Am-241 source with an amplification of 100x (a) and 300x (b). Spectra are obtained from a MCA.

In both graphs of figure 5.1 the noise is clearly visible. In the first part of the spectrum and the last part the intensity is produced by hardware components like the detector and the amplifier. In figure 5.1(a) the 60 [keV] peak is clearly visible, ranging from 1.5 [V] to 4 [V]. In figure 5.1(b) this peak is less intense and divided over a greater range from 6.0 [V] to 9.0 [V]. From these graphs the amplification was set to 100. This choice is made to decrease the influence of the background (see section 5.3). By choosing the amplification of 100 the intensity ratio source/background is kept at a minimum.

5.2 Defining wall

The wall of the pebble-bed is determined as described in section 4.7. For this procedure different measurements were used to see if the results were valid. The data used in figure 5.2 are from the measurements of multisized pebble-bed 3 (complete profile in appendix D.2).

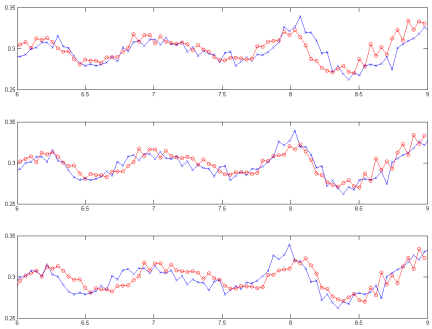

Figure 5.2: Matlab figure used to determine the edge of the pebble-bed

As can be seen in the figure the overlap is visible. Using the MATLAB code the position of the wall is determined. The wall is defined as 1 [mm] away from the data point with the highest void fraction. This results is compatible with the other long time measurements of the unisized (figure 5.8) and shaken experiment (figure 5.10).

5.3 Background

During the project the background is measured several times. At first a energy spectrum is obtained of the background by an amplification of 100x. The counts per channel are presented in figure 5.3 and the method of measuring was the same as mentioned in section 5.1. The used method for calibration provided information about the background as a function of the amount of perspex. A single measurement lasted 10 minutes leading to an uncertainty between 2.5 and 3.0%. The results can be seen in figure 5.4. Day-long measurements were made to check the background over time. The first time was in the begin of June while the reactor was active. The second time was halfway through July while the reactor was inactive for a week. The measurements are shown in figure 5.5. For both experiments the uncertainty is 2.5% due to the maximum amount of pulses of 1500.

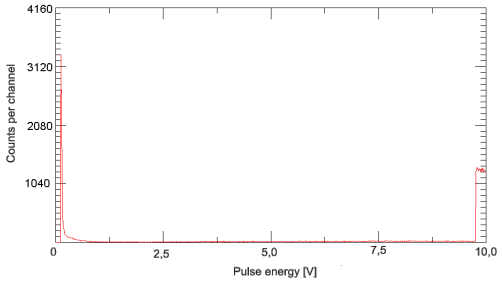

Figure 5.3: Energy spectrum of the background with an amplification of 100. Spectrum is obtained from a MCA.

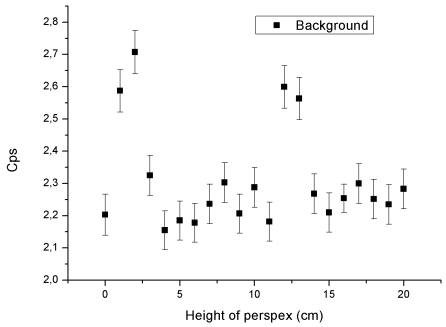

Figure 5.4: Measured background during calibration experiment

As can be seen in figure 5.3 the background does not hold specific energy levels. The counts on the beginning and the end of the spectrum are produced by the used hardware. By choosing a correct filter it is important to avoid this regions. According to figure 5.4 the amount of perspex does not influence the background. A few measurements are incompatible to the rest. These differences are probably produced by the time of measuring. The calibration measurements were made in two days. The second day was started with a perspex height of 12 cm. A second possibility is that the source was in the neighborhood of the detector which led to more counts.

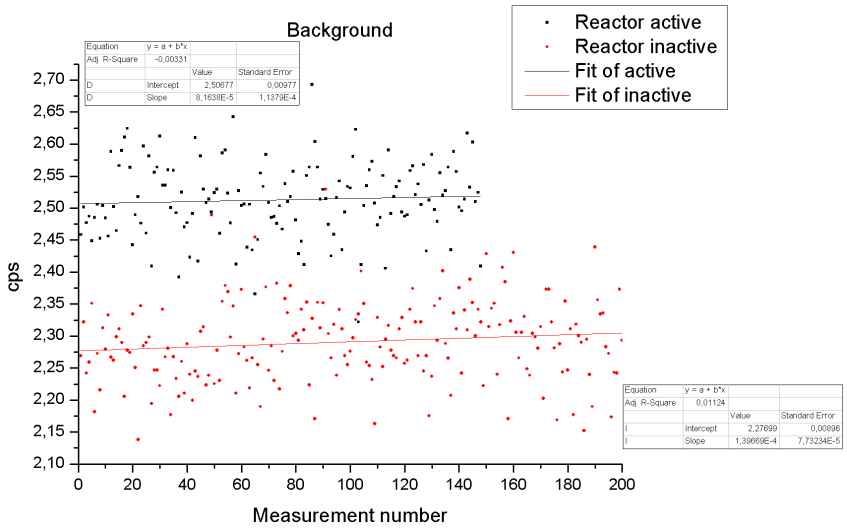

Figure 5.5: Two day-long measurements of the background

The results of the day-long measurements are shown in figure 5.5. Fits are made to simulate the background for the void fraction measurements. The difference between an active/inactive reactor amounts to 0.23 counts per second. During one experiment the background is quite steady but the results of the two experiments

do not overlap at all. This is probably caused by the absence of active rest products in an inactive reactor. The steady background implies that the background can be simulated as a constant value. During all void fraction experiments the reactor was active. That's why the background is simulated as a constant value of 2.51 ± 0.02 counts per second.

5.4 Calibration

Measurements were made to validate the experimental setup. This is done as described in section 4.3. In figure 5.6 the decrease in intensity is seen as a function of adding more disks. Figure 5.7 shows the packing fraction according to the measurements (with and without background correction) and theory.

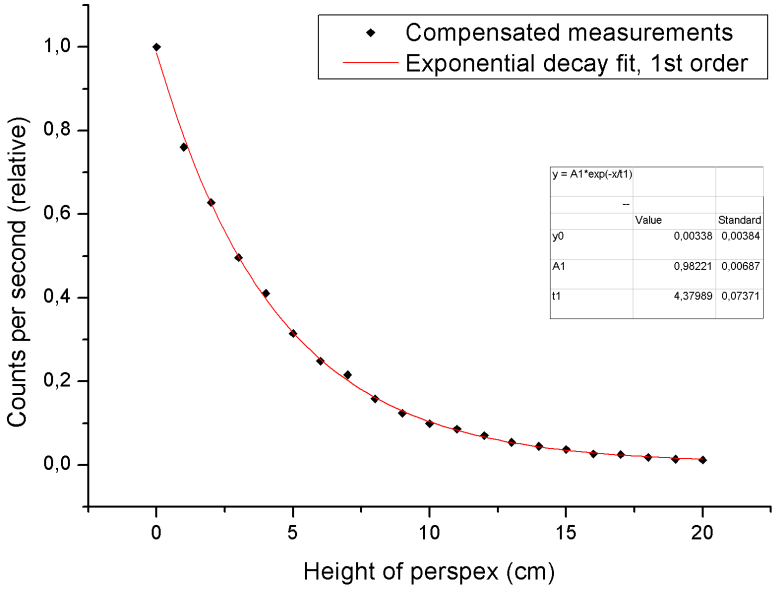

Figure 5.6: Relative intensity obtained from count rate measurements by using 10 [mm] acrylic disks. First order exponential decay fit is performed to calculate the attenuation coefficient of acrylic.

From the exponential fit in figure 5.6 the attenuation coefficient of acrylic at 60 [keV] can be calculated. The attenuation coefficient of $1/t_1 = 0.2288 \pm 0.004$ [cm^{-1}], is in close agreement with the theoretical value of 0.2285 [cm^{-1}] [18].

The packing fraction at different values of the perspex height can be calculated from the relative intensity by using the calibration method, equation 2.5. In figure 5.7 three lines are visible. The black/cube line is the packing fraction of the intensity not compensated for background. The red/circle line is compensated for the measured background. The blue/triangle line is the actual packing fraction of the height of perspex. After compensating the signal for the measured background,

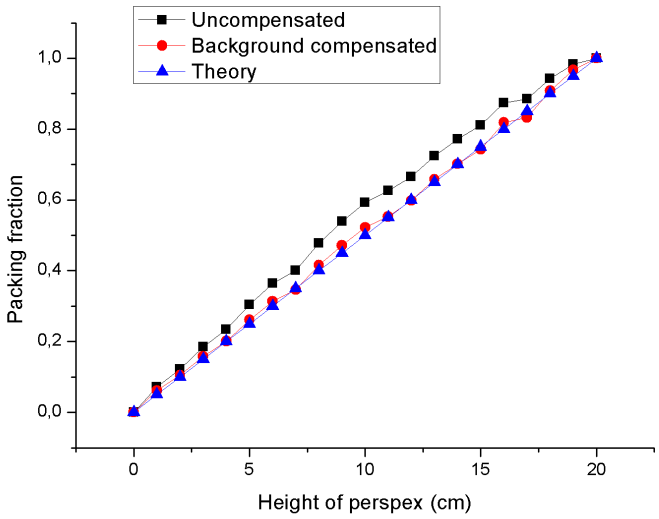

Figure 5.7: Packing fraction of 10 [mm] disks calculated from count rate measurements

the measured packing is in agreement with the calculated packing. This result is compatible with the results of Van Dijk, although he had after compensation still a little difference between the red and blue line possibly caused by build-up. A probable reason for this conflict could be different hardware settings. Another possibility is a difference in measurement time which has influence on the uncertainty. This calibration measurements have an uncertainty around 1.0% while the uncertainty of Van Dijk is unknown. According to figure 5.7 no extra compensation is needed if the background at each point is well-known.

5.5 Experiment 1: Unisized pebble-bed

Firstly a measurement was performed to compare results to earlier studies. The experiment was done with a total of 5457 +/- 10 pebbles. The experiment as shown in figure 5.8 last six measurement days. This is mainly caused by the use of the smaller collimator, reducing the intensity by 80% . The minimum amount of counts for one measurement was set to 5000. The uncertainty per measurement point is relatively high but due to the high density of measurement points the behavior of the profile is still visible.

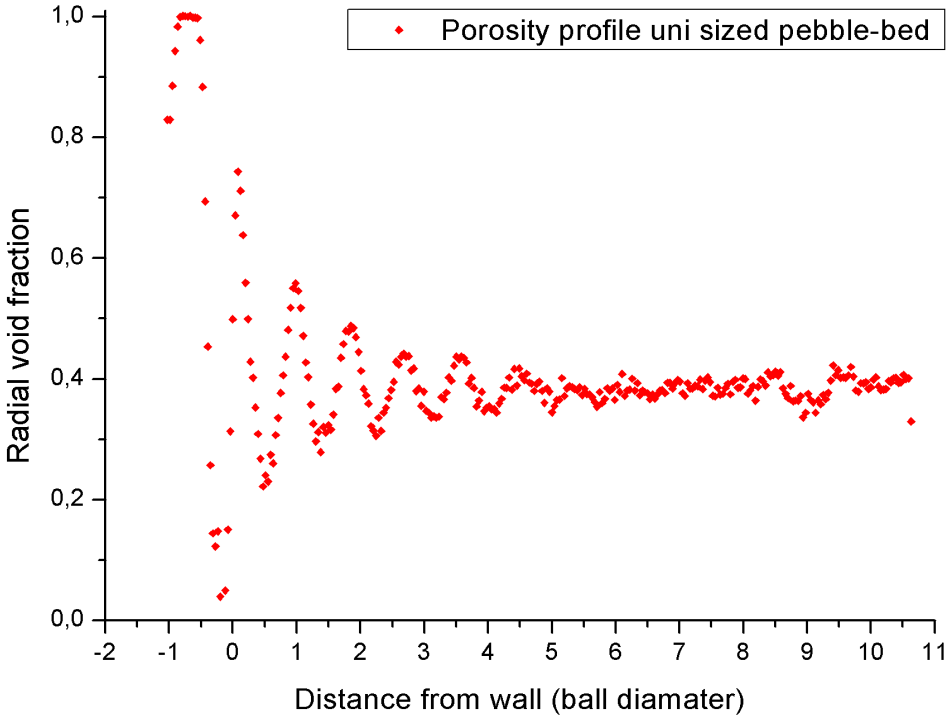

Figure 5.8: Porosity profile of an unisized pebble-bed

The experiment is started one ball diameter from the inner wall. In these measurements the calibration of only air is visible by a void fraction of 1.0. Subsequently the intensity through the wall is measured leading to a decrease of the void fraction. Because of the overlap between wall and pebble stacking the transition is not perfect. The end of the wall is defined as described in section 5.2. From here on the oscillatory behavior is clearly visible. In about 5 sphere diameters the void fraction damps out to an average of 38%. The center of the pebble-bed can also be seen at 9 diameters from the wall. The void fraction is measured locally at these points leading accidental to a lower packing fraction. In figure 5.9 the data obtained from this experiment is compared to other research of Mueller [16] and Benenati [12]. The results agree with theory which means that the experimental setup is working fine.

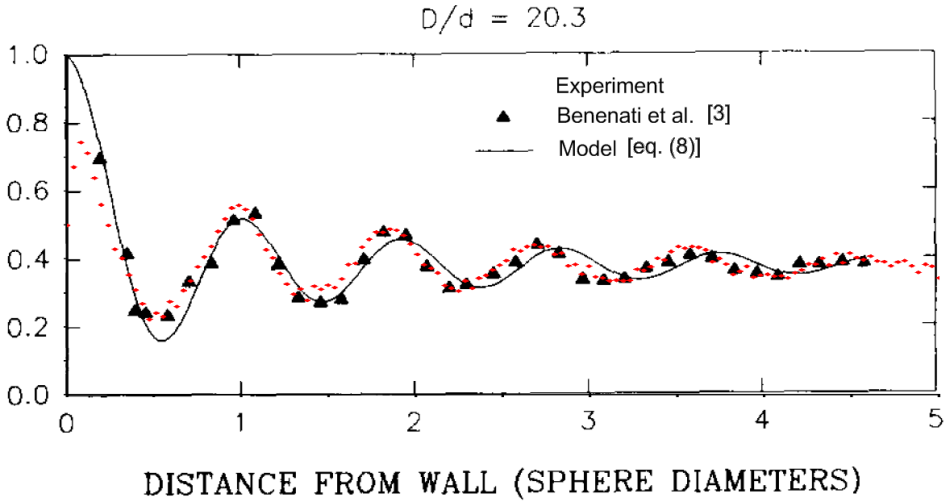

Figure 5.9: Radial porosity profile of the pebble-bed. The data from this experiment is compared to the results of Mueller and Benenati.

Influence smaller collimator The uncertainty increases when using the smaller collimator. This is caused by the intensity decrease of the source. This will not only lead to a longer measurement time but will cause more problems. The first problem is the signal to noise ratio. Using a smaller collimator drastically decrease this ratio. When measuring through the wall of the pebble-bed the detected signal with background is about 3.0 counts per second. With a simulated background of 2.5 counts per second the ratio is 0.2, five times as much background as useful signal.

The second problem is the calibration method. A reliable calibration is an important criterion of this method. The average void fraction is totally dependent on this calibration method. Using the small collimator the calibration of a fully filled pebble-bed will not be as trustworthy as required. The uncertainty in the unisized experiment was on average 10%. This high uncertainty is not compensated by the increase in resolution. In the following measurements the 2 [mm] collimator is used to reduce this uncertainty while the resolution of the experiment is still sufficient.

5.6 Experiment 2: Shaken pebble-bed

Measurements were performed to investigate the influence of shaking the pebble-bed. The pebble-bed was shaken as described in section 4.4.1. The results of the experiment can be found in figure 5.10. The experiment was done with a total of 5457 +/- 10 pebbles. To obtain the data for this experiment four measurement days were required. The 2 [mm] collimator was used and the minimum counts per measurement point was set to 7500.

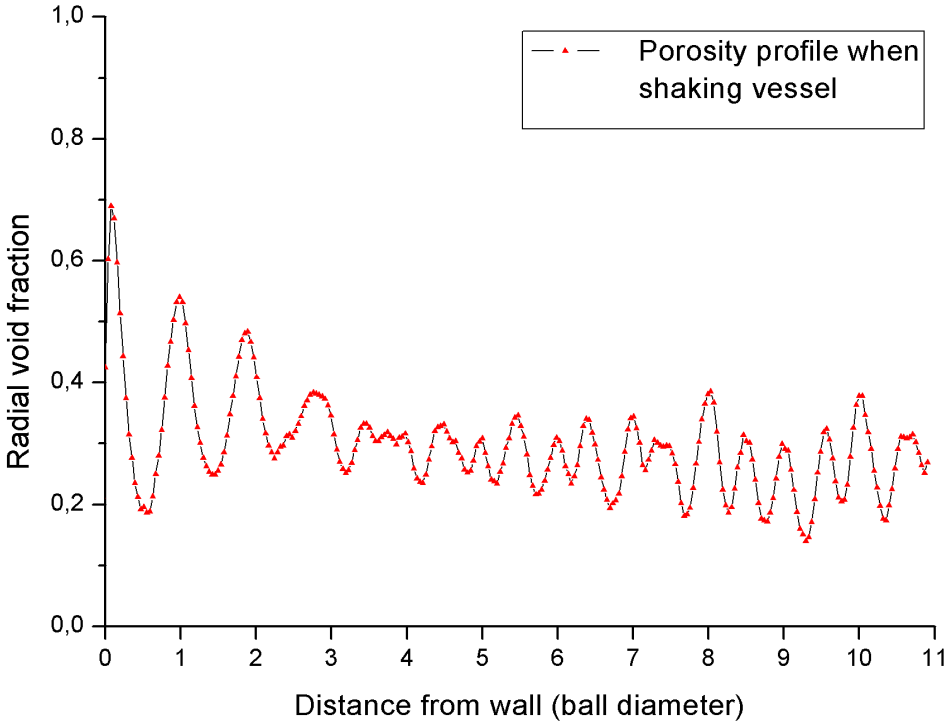

Figure 5.10: Porosity profile of a shaken bed

As can be seen in figure 5.10 shaking the vessel has a significant influence on the porosity profile of the bed. It seems like this method of filling the vessel puts the spheres in a specific structure. In the beginning the profile follows the profile of a unisized profile. After two diameters inside the vessel the void fraction decrease dramatically and keep oscillating in an irregular sequence. In the middle of the bed, around 9 diameters, it can be seen that the void fraction is repeating itself. At exactly 9 diameters from the wall, the void fraction is measured locally because this is the center of the pebble-bed. Rotating the vessel has no influence on the part of ht vessel between source and detector. The measurements points at 8 and 10 diameters and further away from the middle, show the same tendency meaning that the profile is reproducible.

5.7 Experiment 3,4,5: Multisized pebble-bed

Experiments were performed with different multisized pebble stackings. The 2 [mm] collimator was used and the minimum counts per measurement point was set to 7500. As described in section 4.4.1 it is difficult to realize a ideally pebble stacking. In the first part of this section the differences in the setups will be discussed. In the second part the results will be presented.

5.7.1 Obtained pebble-bed stackings

Three pebble-bed stackings were made and are shown in figure 5.11. The amount of pebbles used in each setup can be found in table 5.1.

Bed No.	12.7 [mm]	3.18 [mm]
3	5450	30.000
4	5325	30.000
5	5450	30.000

Table 5.1: Number of pebbles used in each experiment

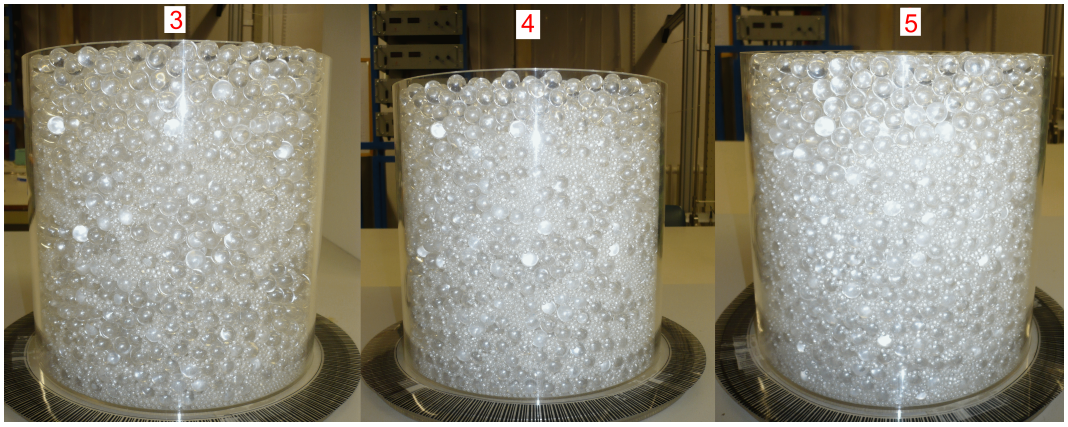

Figure 5.11: Three different multisized pebble stackings used in the radial void fraction measurements

Pebble-bed 3 In pebble-bed 3 the small spheres were put at random in the vessel. As can be seen in figure 5.12(a) this results in an imbalanced distribution throughout the vessel. Their are places where the smaller pebbles are concentrated and where the pebbles are absent.

Pebble-bed 4 In the second multisized pebble-bed the small pebbles were mostly put at the edge of the vessel. The outcome of this method was that less big spheres

could be used. The smaller pebbles fully replaced the bigger ones at the edge of the pebble-bed as can be seen in figure 5.12(b). The smaller spheres are filling up most of the holes between the bigger spheres.

Pebble-bed 5 For pebble-bed 5 the technique formulated in section 4.4.1 was used. This results in an almost uniform distribution of smaller pebbles in the vessel. Just like in pebble-bed 4 the smaller pebbles were put mostly within 5 sphere diameters of the wall. The spheres, not used in pebble-bed 2, were brought back in the vessel due to the different method of filling. The result of this method of filling was a better distribution between the smaller en bigger spheres. Still it is not ideal because at the top of the bed the smaller spheres are not present as can be seen in figure 5.11.

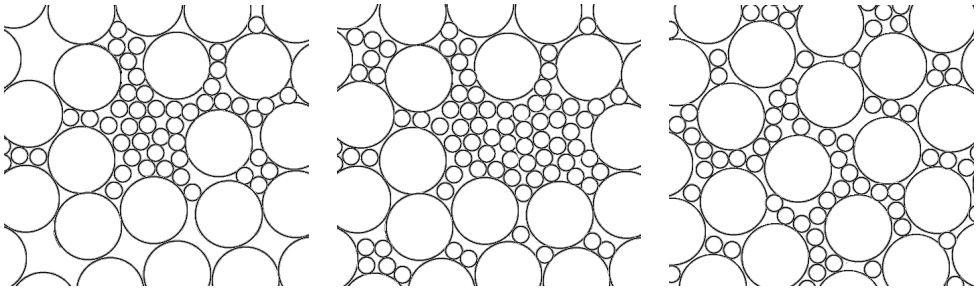

(a) Experiment 3 (b) Experiment 4 (c) Experiment 5

Figure 5.12: A sketch of the multisized pebble stackings. The pebble distributions are made in the near wall region.

5.7.2 Results

The results of the measurements are shown in figure 5.13. The three different multisized pebble stackings (blue, red and green) are plotted together with the results of the unisized pebble-bed of section 5.5. The uncertainty varies from 1% at high void fraction measurements to 6 % for places with a high perspex fraction. The porosity profiles of the multisized pebble-beds is significantly lower than the unisized case. This behavior is expected because the volume of acrylic in the multisized beds is increased so the void fraction should be lower. Notable is the fact that in all three cases the void fraction is shifted downwards in the whole range. This decrease is larger than expected. With 30,000 extra pebbles the void fraction should decrease with only 0.05. In figure 5.13 the shift is more than 0.1. The influence of the calibration measurements mostly determine the average void fraction.

The oscillatory behavior of a porosity profile remains visible, hardly not reducing the flow channeling. Further more, the damping factor of the void fraction in multi bed 2 is stronger than in multi bed 3. This difference is probably caused by the method of

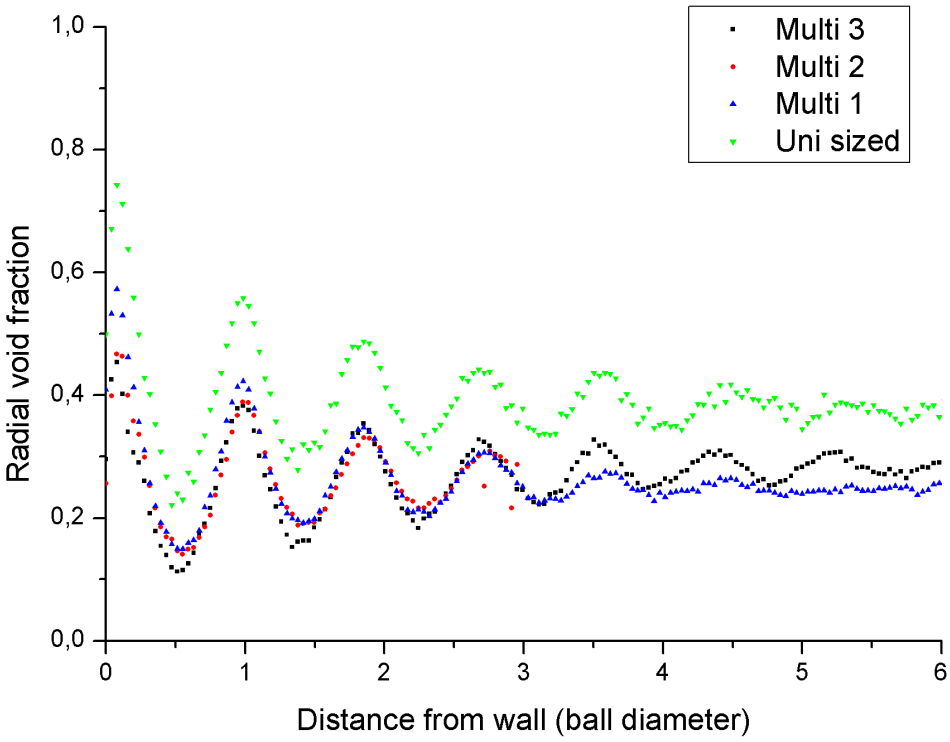

Figure 5.13: Porosity profiles of different multisized pebble stackings 5.11 compared to the profile of an unisized pebble-bed 5.8

filling the vessel. For the last pebble stacking, the bed was slightly shaken resulting in more oscillations as can be seen in the results of section 5.6. Because the vessel was mostly filled at the edge of the bed it is not surprising that the void fraction is approximately 12% lower than in the unisized bed. This is most clearly visible in the data of bed 3 (black/cube line) where the void fraction is brought to a minimum of 10% at an half diameter from the wall.

Chapter 6

Conclusions

6.1 Conclusions

Gamma-ray tomography was used to determine the radial void fraction of a pebble-bed. This porosity profile was measured for different kinds of pebble-beds. The profile of a bed with one size of spheres confirmed earlier studies. The porosity profile of the shaken bed showed a oscillatory behavior not seen before. At what extent this shaken bed simulates a earthquake shaken pebble-bed is unknown. The multisized pebble-bed with spheres of two sizes were difficult to produce. The overall void fraction of this beds was significant lower than the unisized packed bed. Mixing the smaller spheres in the bed slightly decreased the amplitude of the oscillations. Flow channeling will probably still be observed in a multisized bed.

The average void fraction was lower than expected. This could be caused by differences in the background. As long as the background radiation during an experiment can be measured the influence on the average void fraction is kept at a minimum. Another topic of interest is the calibration method. The vessel is made of the same material as the spheres but still differences in the two substances could lead to an incorrect calibration method.

An method is developed to determine the walls boundary. It is defined as the point with an distance of 1 [mm] from the point of highest void fraction in the profile. This definition was proven useful according to the experiments. The smaller collimator increases the resolution slightly. However, the increase in uncertainty made the results less reliable as expected. This is mostly caused by an bad signal-to-noise ratio and an questionable calibration method. After this first experiment and conclusion the 2 [mm] collimator is used in the other experiments.

6.2 Recommendations

In the first part of this section, I will provide some recommendations for improvements of the PebBEx facility that would be beneficial to the measurements. The second part will consist of topics for follow-up research.

6.2.1 Experimental recommendations

Background measurement The background radiation influences the result of the average void fraction. As has been stated the background should not be simulated as a constant factor but must be measured at the same time in an experiment to determine the average void fraction more precise.

Calibration method Another possibility which caused a low void fraction is the calibration method. Perhaps a correction is needed to compensate for the material differences between vessel and spheres. A second recommendation is to increase the measurement time for the calibration measurements. This could be achieved by improving the Labview program.

Setup rotation The method of rotating the pebble-bed is not always reliable. In the setup different O-rings were used during the variety of experiments. The rings can only be used temporary due to the tensions caused by the weight of the pebble-bed. Changing the motor belt so that the rotation is more trustworthy would be highly recommended.

Mounting of the source The intensity of the beam is influenced by the mounting of the source. The measurement time can be decreased by searching the position with the maximum amount of signal. It is recommended to build a new mounting device to keep the source at this position.

6.2.2 Follow-up research

Reproducibility Extra measurements can be performed to validate the presented results of this thesis. Especially the porosity profile of a shaken bed should be measured in detail to confirm the effect of an earthquake.

Mixing more different types of pebbles With the results and setup at hand porosity experiments can be done on spheres with other dimensions or shapes. The ratio of the used spheres can be varied to determine ratio which reduced the oscillatory behavior most. Experiments can also be performed with unisized larger diameter spheres to see the influence of the diameter ratio of vessel/sphere on the radial void fraction.

Pressurizing the bed The influence of pressurizing the bed can be investigated more severely. The method to create a uniform surface did not visibly led to pressurizing the bed. Measurement can be performed to justify this observations.

Method for filling the vessel It turns out that a regular distribution of a multi-sized pebble packing is hard to realize. The method of filling the bed can be changed to research the influence of different filling methods. A method could be developed do achieve a more ordered pebble stacking.

Bibliography

[1] The 6 fourth generation reactors: http://www.world-nuclear.org/info/inf77.html (2009).

[2] HTTR: http://httr.jaea.go.jp/eng/index_main_eng.html

[3] GTMHR: http://gtmhr.ga.com/index.html

[4] Z. Wu, D. Lin and D. Zhong: The design features of the HTR10 *Nuclear Engineering and Design*, 218 (2002) p. 25.

[5] PBMR: http://www.pbmr.com/

[6] TRISO particles: http://www.romawa.nl/nereus/fuel.html

[7] A. Ooms. Pebble flow in a high temperature reactor. Master's thesis, Delft University of Technology, (2008).

[8] E. Webbe. Multi sized pebble stacking. Bachelor's thesis, Delft University of Technology, (2009).

[9] V. van Dijk. Radial void fraction measurement of a randomly packed pebble-bed. Bachelor's thesis, Delft University of Technology, (2008).

[10] W. W. Schertz, K. B. Bischoff: Thermal and Material Transport in Non-isothermal Packed Beds *AIChE Journal*, 15 (1969) p. 597.

[11] S. M. White and C. L. Tien: Analysis of flow channeling near the wall in packed beds *Wärme-Stoffübertragung*, 21 (1987) p. 291.

[12] R. F. Benenati and C. B. Brosilow: Void Fraction Distribution in Beds of Spheres *AIChE Journal*, 8 (1962) p. 359.

[13] D. Bedenig: Experimentelle Untersuchungen in Stromungsverhalten eines Kugelhaufens im Hinblick auf den Brennelementkreislauf im Core eines Kugelhaufenreactor, Institut fur Reaktorentwickelung Kearnforschungsanlage, Julich, Germany (1966).

[14] K.K. Pillai: Voidage variation at the wall of a packed bed of spheres *Chem. Eng. Sci.*, 32 (1977) p. 59.

[15] J.S. Goodling, R.I Vachon, W.S. Stelpfug, S.J. Ying and M.S. Khader, *Powder Technology*, 35 (1983), p. 23.

[16] G.E. Mueller, *Powder Technology*, 72 (1992), p. 269.

[17] Am-241: http://www.stuarthunt.com/Downloads/RMSDS/Am241.pdf

[18] PMMA: http://physics.nist.gov/PhysRefData/XrayMassCoef/ComTab/pmma.html

[19] Brouwer e.a.: Praktische stralingshygiëne (2008).

[20] C.G. du Toit: The numerical determination of the variation in the porosity of the pebble-bed core, Potchefstroom University for CHE, South Africa (2002).

Appendix A

X-ray mass attenuation coefficients of PMMA

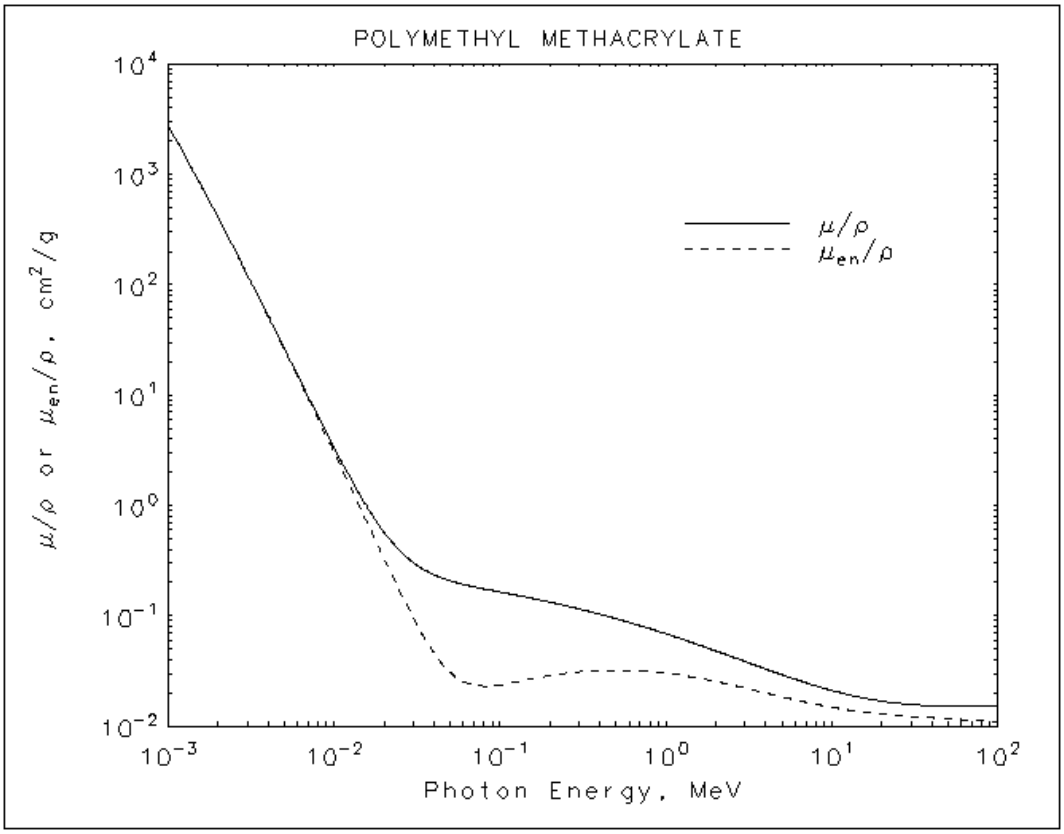

Figure A.1: X-ray mass attenuation coefficients of PMMA

Appendix B

Decay scheme Am-241

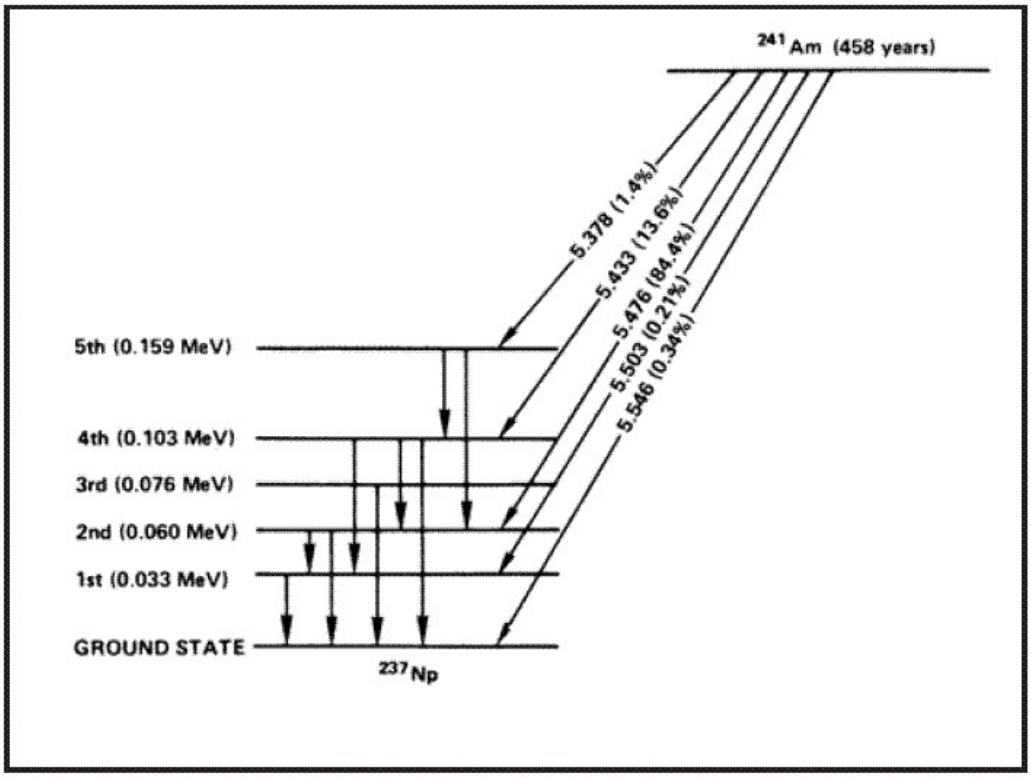

Figure B.1: Decay scheme of Americium-241

Appendix C

Hardware

Ortec 270

ORTEC®

570
Amplfier

- **General-purpose amplifier for energy spectroscopy with all types of detectors**
- **Unipolar output**
- **Low noise, wide-gain range and front-panel selectable time constants**
- **Gated BLR with automatic threshold control for excellent counting rate performance**

The ORTEC Model 570 Amplifier is a general-purpose spectroscopy amplifier that offers excellent performance for varying counting rates at an economical price.

The low noise, wide-gain range and selectable shaping networks make this instrument ideally suited for operation with semiconductor detectors, proportional counters, and scintillation detectors in a wide variety of high-resolution spectroscopy applications.

The Model 570 incorporates an automatic gated baseline restorer, which causes the system resolution to be nearly independent of input counting rates. Figure 1 illustrates the peak shift and resolution for a typical gamma spectroscopy system.

The gated baseline restorer (BLR) includes a discriminator that operates the sensing circuits that normally establish the baseline reference for the MCA.

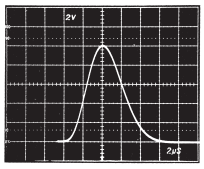

2 V/cm, 2 µs/cm

UNIPOLAR OUTPUT

Performance of the spectrometer often depends on the precision of the setting of the BLR threshold. The Model 570 offers the convenience of an automatic threshold control, which typically gives as good or better results than those the most experienced operator could achieve manually.

The active filter networks of the Model 570 generate a very symmetrical unipolar output with optimal signal-to- noise ratio over a wide range of time constants.

The excellent dc stability of the Model 570 output eliminates spectrum broadening caused by dc drift and ensures that the high-resolution capability of germanium detectors is realized.

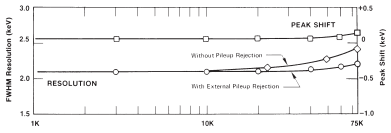

Fig. 1. Typical Resolution and Baseline Stability vs. Counting Rate for the Model 570 in a Gamma Spectroscopy System.

570
Amplfier

Specifications

PERFORMANCE

GAIN RANGE Continuously adjustable from 1 to 1500.

PULSE SHAPE Semi-Gaussian on all ranges with peaking time equal to 2.2τ and pulse width at 0.1% level equal to 2.9 times the peaking time.

INTEGRAL NONLINEARITY For 2-µs shaping time, <±0.05%.

NOISE Typically <5 µV for unipolar output referred to the input, using 2-µs shaping and Coarse Gain ≥100.

TEMPERATURE INSTABILITY
Gain ≤±0.0075%/°C, 0 to 50°C.
DC Level ≤±50 µV/°C, 0 to 50°C.

BIPOLAR CROSSOVER WALK ≤±3 ns at 0.5 µs for 50:1 dynamic range, including contribution of an ORTEC Model 552 Single-Channel Analyzer.

OVERLOAD RECOVERY Recovers to within 2% of rated output from X300 overload in 2.5 nonoverloaded pulse widths using maximum gain for Unipolar Output.

SPECTRUM BROADENING Typically <16% FWHM for a ^{60}Co 1.33 MeV gamma line at 85% of full scale for an incoming count rate of 1 to 75,000 counts/s (Unipolar Output, 2-µs shaping).

SPECTRUM SHIFT Peak position shifts typically <0.024% for a ^{60}Co 1.33-MeV gamma line at 85% of full scale measured from 1 to 75,000 counts/s (Unipolar Output, 2-µs shaping).

CONTROLS

FINE GAIN 10-turn precision potentiometer with graduated dial for continuously variable direct-reading gain factor of X0.5 to X1.5.

COARSE GAIN 6-position switch selects feedback resistors for gain factors of 20, 50, 100, 200, 500, and 1k. Jumper on the printed wiring board (PWB) selects X0.1 attenuation.

INPUT POLARITY Locking toggle switch selects either Pos or Neg input pulse polarity.

SHAPING TIME 6-position switch selects time constants for active pulse-shaping filter network from 0.5, 1, 2, 3, 6, and 10 µs.

PZ ADJ Screwdriver adjustable potentiometer to set the pole-zero cancellation to compensate input decay times from 40 µs to ∞.

BLR 3-position locking toggle switch selects the source of control for the gated baseline restorer discriminator threshold from:
Auto The BLR threshold is automatically set to an optimum level, as a function of the signal noise, by an internal circuit.
PZ Adj The BLR threshold is determined by the threshold potentiometer. The BLR time constant is also greatly increased to facilitate PZ adjustment; this position may give the lowest noise for count rates under 5000 counts/s and/or longer shaping times.
Threshold The BLR threshold is manually set by the threshold potentiometer.

DC Screwdriver adjustable potentiometer to set the Unipolar Output dc level; range ±100 mV.

INPUT

INPUT Front-panel BNC connector accepts either positive or negative pulses with rise times of 10 to 650 ns and decay times of 40 µs to ∞, Z_{in} = 1000 Ω dc-coupled; linear maximum 10 V; absolute maximum 20 V.

OUTPUTS

UNIPOLAR Front-panel BNC connector with Z_0 <1 Ω, short-circuit proof; prompt with full-scale linear range of 0 to +10 V; active filter shaped; dc-restored; dc-level adjustable to ±100 mV.

PREAMP POWER Rear-panel standard ORTEC power connector. Amphenol 17-10090, mates with captive and noncaptive power cords on all ORTEC pre-amplifiers.

BUSY OUTPUT Rear-panel BNC connector with Z_0 <10 Ω provides a +5 V logic pulse for the duration that the input pulse exceeds the baseline restorer discriminator.

ELECTRICAL AND MECHANICAL

POWER REQUIRED +12 V, 60 mA; –12 V, 30 mA; +24 V, 80 mA; –24 V, 85 mA.

WEIGHT
Net 1.5 kg (3.3 lb).
Shipping 3.1 kg (7.0 lb).

DIMENSIONS Standard single-width NIM module 3.43 X 22.13 cm (1.35 X 8.714 in.) per DOE/ER-0457T.

Ordering Information

To order, specify:

Model	Description
570	Amplifier

Specifications subject to change
122807

ORTEC®
www.ortec-online.com
Tel. (865) 482-4411 • Fax (865) 483-0396 • ortec.info@ametek.com
801 South Illinois Ave., Oak Ridge, TN 37831-0895 U.S.A.
For International Office Locations, Visit Our Website

AMETEK®
ADVANCED MEASUREMENT
TECHNOLOGY

Canberra Model 2030

CANBERRA

Features

- Independent ULD, LLD, and SCA outputs
- Precise threshold discrimination
- Exceptional stability – dc-coupled input
- External baseline sweep input
- Dynamic range 1000:1
- LLD monitored by LED display
- Source matched logic outputs

Model 2030
Single Channel Analyzer

Description

The CANBERRA Model 2030 analyzes the peak amplitude of energy pulses from nuclear pulse shaping amplifiers, and generates its primary logic output (SCA) for input analog pulses between the levels referenced by the Lower Level (E) and Window (ΔE) front panel ten-turn controls. Auxiliary outputs from the Lower Level Discriminator (LLD) as set by (E), and the Upper Level Discriminator (ULD) as set by (E + ΔE) are also provided. Timing of these logic outputs is set as the trailing edge of the input signal crosses the (E) reference.

The several outputs may be used together or individually to assist in a wide variety of applications from simple noise removal to extraction of a narrow energy range from a wide spectrum of signals for energy analysis. The sharp, precise threshold discrimination levels are exceptionally stable (drift is less than ±0.005%/°C, full scale). The dc coupled input allows excellent baseline stability limited only by the shaping amplifier's restorer. These significant features permit excellent amplitude discrimination, even in high count rate spectra.

The Lower Level (E) threshold is calibrated by reference to the regulated NIM supply voltages, and is usable over the range from +0.001 V dc to +10.0 V dc. Linearity of control is limited only by the specified ±0.25% maximum nonlinearity of the front panel potentiometer. A front panel mounted LED is useful in visually monitoring the setting of the Lower Level (E) reference just above the shaping amplifier's noise level (the LED will fade off).

The Window (ΔE) threshold is also calibrated by reference to the regulated NIM supply voltages, and is usable over the range from the Lower Level (E) setting to +10.0 V dc. A front panel ΔE Range switch allows use of a 1.0 V full scale range for very fine adjustments of the desired window.

An external lower level discriminator (LLD) input on the rear panel may be used in place of the front panel control for applications requiring a ratioed or sweeping baseline reference over the energy range. This input requires a positive polarity reference voltage, and is linear over the full scale of 0 to +10.0 V dc. A locking toggle switch is used to select this input.

All output logic signals are positive logic, and are adjustable in peak amplitude for compatibility with interfacing instruments. All outputs are source matched with 50 Ω series resistive terminations to prevent ringing due to reflections on unterminated cables, and the resulting multiple counting frequently experienced. The instrument is shipped with a socketed resistor which limits the output to +5 V nominal (open circuit) for direct interface with common TTL circuitry. The resistor (1 for each output) can be removed to obtain a

Phone contact information

Benelux/Denmark (32) 2 481 85 30 • **Canada** 905-660-5373 • **Central Europe** +43 (0)2230 37000 • **France** (33) 1 39 48 52 00 • **Germany** (49) 6142 73820
Japan 81-3-5844-2681 • **Russia** (7-495) 429-6577 • **United Kingdom** (44) 1235 838333 • **United States** (1) 203-238-2351

For other international representative offices, visit our web site: **http://www.canberra.com** or contact the CANBERRA U.S.A. office.

NSP0100 2/07 Printed in U.S.A.

Model 2030 Single Channel Analyzer

+8 V nominal open circuit voltage for instruments requiring the NIM pulse level, or +4 V nominal into the 50 Ω load termination which some other instruments provide. This flexibility adapts the output signal to various needs without risking the problem encountered with improperly driven cables. Load end terminations are not necessary.

Careful attention has been paid to minimize reflections of the fast logic pulses back to the analog input. Thus all logic outputs are isolated from chassis to prevent circulating pulse currents in the instrument bin.

Specifications

INPUTS
- SIGNAL INPUT – Accepts +0.01 to +10.0 V dc, unipolar or bipolar (positive lobe leading) pulses from shaping amplifier. Z_{in} = 1 kΩ. Shaping time constant range 0.1 to 20 µs; front and rear panel BNCs.
- EXTERNAL LLD REFERENCE – Accepts 0 to +10.0 V dc; Z_{in} = 1 kΩ; rear panel BNC.

OUTPUTS
- SCA – Positive logic +5 V nominal pulse amplitude, adjustable to +8 V nominal pulse by removing socketed resistor; Z_{out} = 50 Ω; pulse width 0.5 µs, nominal; rise time and fall time <25 ns; front and rear panel BNCs.
- ULD – Same characteristics as SCA output; rear panel BNC.
- LLD – Same characteristics as SCA output; rear panel BNC.

CONTROLS
- LOWER LEVEL (E) – Front panel ten-turn locking dial potentiometer to set lower discriminator threshold level.
- WINDOW (ΔE) – Front panel ten-turn locking dial potentiometer to set window width (upper discriminator threshold level above lower level).
- ΔE RANGE – Front panel toggle switch to set full scale range of WINDOW (ΔE) control as +1.0 V dc or +10.0 V dc.
- LLD REF MODE – Rear panel locking toggle switch to select INTernal lower level via front panel control, or EXTernal input.

INDICATOR
- LOWER LEVEL – Front panel LED blinks when input exceeds LLD setting.

PERFORMANCE
- DISCRIMINATOR NONLINEARITY – <±0.25% of full scale.
- DISCRIMINATOR STABILITY – <±0.005%/°C (±50 ppm/°C) of full scale, referenced to NIM class A supply +12 V dc line.
- DISCRIMINATOR RANGE – ≤1000:1.
- DISCRIMINATOR PULSE PAIR RESOLUTION – <0.65 µs.

CONNECTORS
- All signal connectors are BNC type.

POWER REQUIREMENTS
- +12 V dc – 155 mA –12 V dc – 5 mA

PHYSICAL
- SIZE – Standard single width NIM module 3.43 x 22.12 cm (1.35 x 8.71 in.) per DOE/ER-0457T.
- NET WEIGHT – 0.8 kg (1.8 lb).
- SHIPPING WEIGHT – 1.8 kg (4.0 lb).

ENVIRONMENTAL
- OPERATING TEMPERATURE – 0 to 50 °C.
- OPERATING HUMIDITY – 0-80% relative, non-condensing. Meets the environmental conditions specified by EN 61010, Installation Category I, Pollution Degree 2.

Appendix D

Experimental Data

Unisized pebble-bed

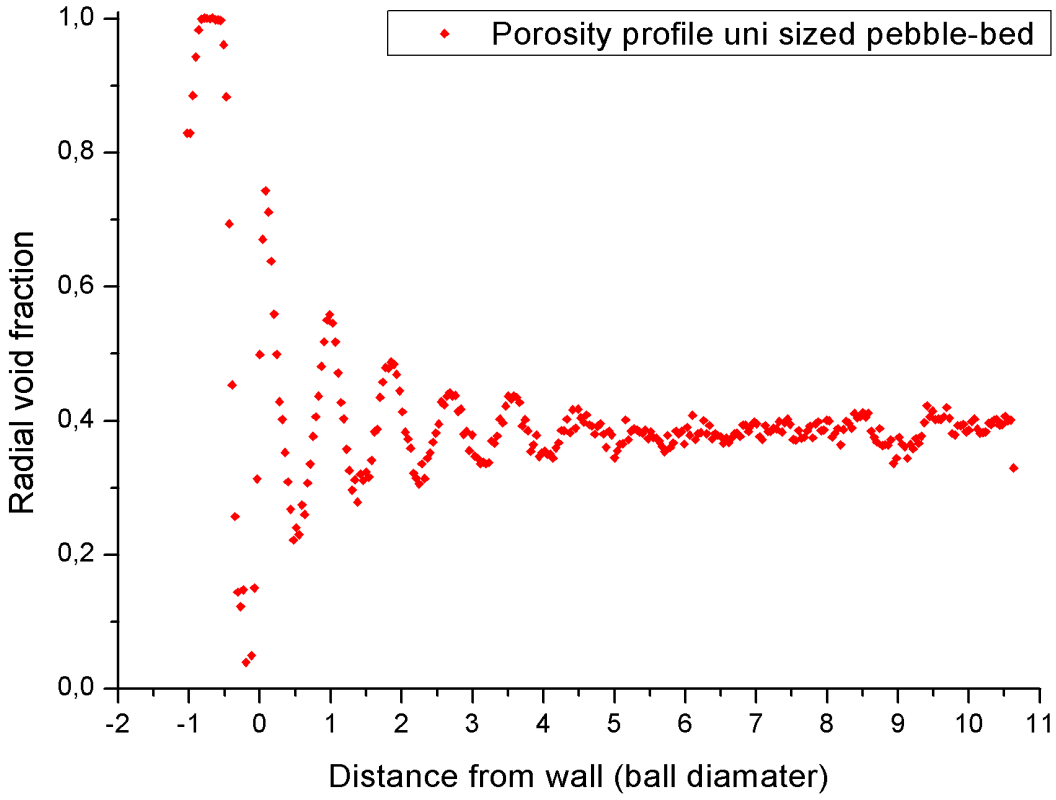

Figure D.1: CAPTION

Multisized pebble-bed

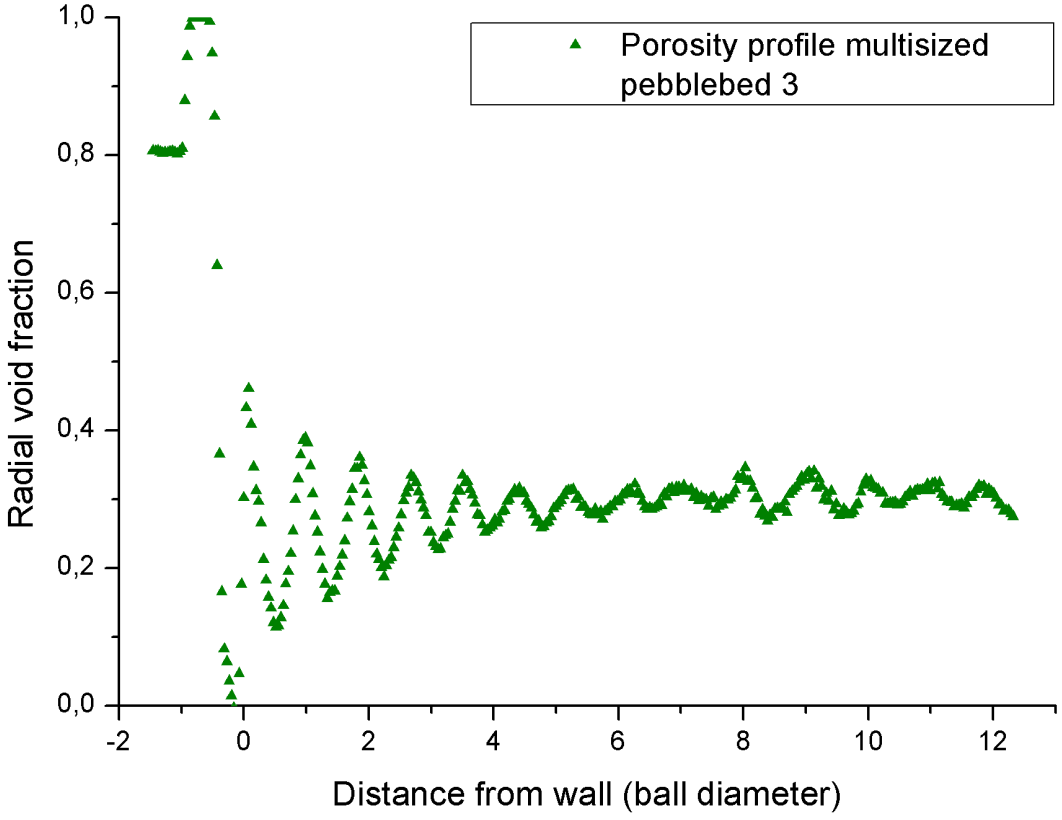

Figure D.2: CAPTION